HEATING LOAD AND COP OPTIMIZATION OF AN IRREVERSIBLE QUANTUM BRAYTON HEAT PUMP WORKING WITH SPIN-1/2 SYSTEMS

Xiaowei Liu[1, 2, 3], Lingen Chen[1, 2, 3*], Fankai Meng[1, 2, 3], Zemin Ding[1, 2, 3]
1 Institute of Thermal Science and Power Engineering, Naval University of Engineering, Wuhan 430033, China;
2 Military Key Laboratory for Naval Ship Power Engineering, Naval University of Engineering, Wuhan 430033, China;
3 College of Power Engineering, Naval University of Engineering, Wuhan 430033, China.
E-mail: lgchenna@yahoo.com; lingenchen@hotmail.com

ABSTRACT

By considering quantum friction, heat resistance and heat leakage, this paper establishes a quantum Brayton heat pump model. The working substance is a two-level spin-1/2 system, and the cycle has four branches: two adiabatic branches and two isomagnetic branches. By using quantum thermodynamics and quantum master equation, this paper obtains heating load and COP of the pump. By using Euler-Lagrange method, this paper optimizes heating load and COP performance for two cases: the general case and the case at high temperature limit. Influences of quantum friction, duration of adiabatic process and heat leakage on the performance are further analyzed.

INTRODUCTION

Heat pumps are important devices which have been used widely and have made great contribution for energy saving. By using finite time thermodynamics (FTT) theory [1-11], a lot of work on performance analysis and optimization have been done, such as endoreversible [12, 13] and irreversible Carnot heat pumps [14, 15], air heat pumps [16, 17], absorption heat pumps [18, 19], thermoelectric heat pumps [20, 21], and so on, and many important and significant conclusions have been obtained. In recent decades, the studies on heat pumps have been extended to microscopic energy conversion systems, such as Brownian heat pumps [22, 23], energy selective electron heat pumps [24, 25], etc. Also, the study on quantum heat pumps has attracted considerable attentions.

Since Scovil and Schultz-Dubois [26] proposed the concept of quantum heat engine, the study on quantum heat engine and quantum refrigerator has attracted more and more interests [27-36]. As for quantum heat pump, Wu et al [37, 38] firstly developed a quantum spin Carnot heat pump model and a

NOMENCLATURE

a , c	[s^{-1}]	Parameter of heat reservoir
B		Heat reservoir
$\vec{B}$	[T]	External magnetic field
C_e		Dimensionless factor which describes magnitude of bypass heat leakage
E_S	[J]	Internal energy of the spin-1/2 systems
$\hat{H}$		Hamiltonian
$\hbar$	[Js]	Reduced Planck's constant
k_B	[J/K]	Boltzmann constant
L_a , L_b , L_c , L_d		Lagrangian functions
$\hat{M}$		Magnetic moment operator
$\hat{N}$		Number operator
n_c		Population of the thermal phonons of the cold reservoir
Q	[J]	Amount of heat exchange
$\hat{Q}_\alpha$, $\hat{Q}_\alpha^+$		Operator in the Hilbert space of the system and Hermitian conjugates
$\dot{Q}_e$	[W]	Rate of heat flow of bypass heat leakage
q		Parameter of heat reservoir
S		Expectation value of spin operator $\hat{S}_z$
$\hat{S}_+$, $\hat{S}_-$		Spin creation and annihilation operators
$\hat{S}(\hat{S}_x, \hat{S}_y, \hat{S}_z)$		Spin operator
T	[K]	Absolute temperature
t	[s]	Time
W	[J]	Work
Special characters		
α		Intermediate variable
β	[J^{-1}]	"Temperature" $\beta = 1/(k_B T)$
γ_+ , γ_-		Phenomenological positive coefficients
λ		Parameter of the heat reservoir
λ_a , λ_b , λ_c , λ_d		Lagrangian multipliers
μ		Friction coefficient
μ_B	[J/T]	Bohr magneton
π	[W]	Heating load
τ	[s]	Time / cycle period
ψ		Coefficient of performance (COP)
ω		"The magnetic field" $\omega = 2\mu_B B(t)_z$
ω_c	[s^{-1}]	Frequency of thermal phonon of cold reservoir
Subscripts		
B		Heat reservoir
c		Cold side
h		Hot side
S		Working substance system
max, $\mu = 0, C_e = 0$		Maximum point for endoreversible case with $\tau_a = \tau_b = 0.01$
1, 2, 3, 4		Cycle states

harmonic Carnot heat pump model, and investigated their performance. Besides quantum Carnot heat pump, the performance of a harmonic Stirling heat pump [28], a quantum spin Ericsson heat pump [39] and an irreversible harmonic Stirling heat pump [40] have also been investigated. Liu et al [41, 42] obtained optimal heating load and COP relation of an irreversible Carnot heat pumps which use, respectively, spin-1/2 systems [41] and harmonic oscillator systems [42] as working substance, and denoted that, for heat loading, the harmonic oscillator heat pump has no maximum while the spin heat pump has.

This paper will develop an irreversible heat pump cycle model and derive its heating load and COP. The working substance is spin system and the cycle is Brayton type. In general case and at high temperature limit, the heating load and COP performance will be optimized, and the influences of quantum friction, duration of the adiabatic processes and heat leakage will be further analysed.

WORKING SUBSTANCE: SPIN-1/2 SYSTEM

(1). The internal energy

Considering a situation that a single spin-1/2 particle is placed in magnetic field $\vec{B}$ whose direction is z axis and changes with time, and the Hamiltonian is given by [43]

$$\hat{H}_{\mathrm{S}} = -\hat{M}\cdot\vec{B} = 2\mu_{\mathrm{B}}\hat{S}\cdot\vec{B}/\hbar = 2\mu_{\mathrm{B}}\hat{S}_z B_z/\hbar = \omega(t)\hat{S}_z/\hbar \qquad (1)$$

where $\hat{S}$, μ_{B}, and $\hbar = h/(2\pi)$ stand for spin angular momentum operator, the Bohr magneton and the reduced Planck's constant, respectively. For simplicity, one refers to $\omega(t) = 2\mu_{\mathrm{B}}B(t)_z$ as "the magnetic field". The internal energy is given by

$$E_{\mathrm{S}} = \left\langle \hat{H}_{\mathrm{S}} \right\rangle = \omega\left\langle \hat{S}_z \right\rangle/\hbar = \omega S/\hbar \qquad (2)$$

where k_{B} stands for the Boltzmann constant and $S = -\hbar\tanh(\beta\omega/2)/2$ is the expectation value of $\hat{S}_z$. For simplicity, one refers to $\beta = 1/(k_{\mathrm{B}}T)$ as the "temperature".

(2). The first law of thermodynamics

As couples thermally to a heat reservoir, the spin-12 system becomes quantum open system. Using Heisenberg picture for change rate of an arbitrary system operator X, one obtains [43]

$$\frac{\mathrm{d}\hat{X}}{\mathrm{d}t} = \frac{i}{\hbar}\left[\hat{H}_{\mathrm{S}},\ \hat{X}\right] + \frac{\partial\hat{X}}{\partial t} + L_{\mathrm{D}}(\hat{X}) \qquad (3)$$

where $L_{\mathrm{D}}(\hat{X})$ is dissipation which originates from thermal system-bath coupling and is given by [27, 44]

$$L_{\mathrm{D}}(\hat{X}) = \sum_{\alpha}\gamma_{\alpha}(\hat{Q}_{\alpha}^{+}\left[\hat{X},\hat{Q}_{\alpha}\right] + \left[\hat{Q}_{\alpha}^{+},\hat{X}\right]\hat{Q}_{\alpha}) \qquad (4)$$

where γ_{α} is phenomenological coefficients which describes the dissipation and is positive, $\hat{Q}_{\alpha}$ and $\hat{Q}_{\alpha}^{+}$ are Hermitian system operators in the Hilbert space.

Substituting $\hat{X} = \hat{H}_{\mathrm{S}}$ into Eq. (3), one obtains

$$\frac{\mathrm{d}E_{\mathrm{S}}}{\mathrm{d}t} = \frac{\mathrm{d}}{\mathrm{d}t}\left\langle \hat{\mathrm{H}}_{\mathrm{S}} \right\rangle = \left\langle \frac{\partial\hat{\mathrm{H}}_{\mathrm{S}}}{\partial t} \right\rangle + \left\langle L_{\mathrm{D}}(\hat{\mathrm{H}}_{\mathrm{S}}) \right\rangle = S\frac{\mathrm{d}\omega}{\mathrm{d}t}\Big/\hbar + \omega\frac{\mathrm{d}S}{\mathrm{d}t}\Big/\hbar \qquad (5)$$

For the spin-1/2 system, one may identify the instantaneous heat flow and power as

$$\dot{Q} = \left\langle L_{\mathrm{D}}(\hat{\mathrm{H}}_{\mathrm{S}}) \right\rangle = \omega\dot{S}/\hbar = \mathrm{d}Q/\mathrm{d}t \qquad (6)$$

$$P = \left\langle \partial\hat{\mathrm{H}}_{\mathrm{S}}/\partial t \right\rangle = \dot{\omega}S/\hbar = \mathrm{d}W/\mathrm{d}t \qquad (7)$$

and identify the inexact differentials of heat and work as

$$\mathrm{d}Q = \omega\mathrm{d}S/\hbar \qquad (8)$$

$$\mathrm{d}W = S\mathrm{d}\omega/\hbar \qquad (9)$$

(3). The change rate of S caused by thermal system-bath coupling

Setting $\hat{X} = \hat{S}_z$, $\hat{Q}_{\alpha}^{+} = \hat{S}_{+} = \hat{S}_x + i\hat{S}_y$ and $\hat{Q}_{\alpha} = \hat{S}_{-} = \hat{S}_x - i\hat{S}_y$ in Eq. (3) and solving the equation, one obtains the change rate of the S as

$$\dot{S} = -a\hbar^2 e^{q\beta_j\omega}[2(1+e^{\beta_j\omega})S + \hbar(e^{\beta_j\omega}-1)] \qquad (10)$$

(4). The adiabatic process

Along the adiabatic process, there is no thermal coupling between spin-1/2 system and heat reservoir. One assumes that

$$\omega(t) = \omega(0) + \dot{\omega}t \qquad (11)$$

where $\omega(0)$ is the initial value of the field and $\dot{\omega}$ is change speed. When $\dot{\omega}$ is not small enough, it will cause quantum non-adiabatic phenomenon [43], and that causes increase of S. From Eq. (8), one obtains that as the S increases, heat generates inside the system and that will cause work dissipation. To describe the influence of that phenomenon, Feldmann and Kosloff [29] introduce a friction

$$\dot{S} = \hbar(\frac{\mu}{t'})^2 \qquad (12)$$

where t' is adiabatic process duration. Using Eqs. (11) and (12), one obtains the S alone the adiabatic process

$$S(t) = S(0) + \hbar(\frac{\mu}{t'})^2 t,\ 0 \le t \le t' \qquad (13)$$

Using Eqs. (5), (11) and (13), one can derive the work done on spin system

$$\begin{aligned} W_{if} &= \int_0^{t'}\mathrm{d}E_{\mathrm{S}} = \frac{1}{\hbar}\int_0^{t'}S\mathrm{d}\omega + \frac{1}{\hbar}\int_0^{t'}\omega\mathrm{d}S \\ &= (\omega_f-\omega_i)(\frac{S_1}{\hbar}+\frac{\mu^2}{2t'}) + \frac{\mu^2(\omega_i+\omega_f)}{2t'} \end{aligned} \qquad (14)$$

The term $\mu^2(\omega_i+\omega_f)/(2t')$ in Eq. (14) is the work dissipation along adiabatic process, and this part of work is the work that done against the quantum friction.

AN IRREVERSIBLE QUANTUM SPIN-1/2 BRAYTON HEAT PUMP MODEL

The heat pump using spin-1/2 system described in above section as working substance. The setup of the heat pump model is given as following:

(1). The external magnetic field: There exists mechanical coupling between a nonzero time-varying external magnetic field and spin system. The field direction is along z axis.

(2). The heat reservoirs: The quantum heat pump absorbs heat from a cold reservoir $\mathrm{B_c}$, and pump heat to a hot

reservoirs B_h. The heat reservoirs both are thermal phonon systems and their temperature β_c and β_h are constants.

(3). The heat pump cycle: The heat pump cycle is composed of four branches: isomagnetic branches $4\to1$ and $2\to3$, and adiabatic braches $1\to2$ and $3\to4$, as displayed in Fig. 1.

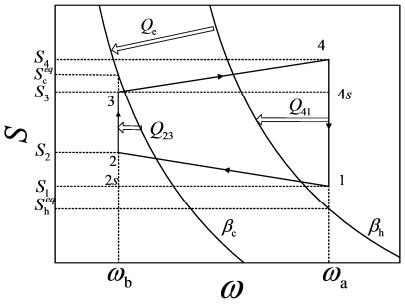

Figure 1 The $S-\omega$ diagram of an irreversible quantum spin-1/2 Brayton heat pump

The heat exchanges for branches $4\to1$ and $2\to3$ can be calculated by using Eq. (8) as

$$Q_{41}=-\frac{1}{\hbar}\int_1^4\omega\mathrm{d}S=\frac{1}{\hbar}\omega_a(S_4-S_1)=0.5\omega_a[\tanh(\beta_1\omega_a/2)-\tanh(\beta_4\omega_a/2)] \tag{15}$$

$$Q_{23}=\frac{1}{\hbar}\int_2^3\omega\mathrm{d}S=\frac{1}{\hbar}\omega_b(S_3-S_2)=0.5\omega_b[\tanh(\beta_2\omega_b/2)-\tanh(\beta_3\omega_b/2)] \tag{16}$$

For the two adiabatic braches, using Eq. (13) and setting $t'=\tau_a$ and $t'=\tau_b$ for processes $3\to4$ and $1\to2$, one obtains

$$S_4=S_3+\hbar\mu^2/\tau_a \tag{17}$$

$$S_2=S_1+\hbar\mu^2/\tau_b \tag{18}$$

Using Eqs. (17), (18) and $S=-0.5\hbar\tanh(\beta\omega/2)$, one obtains

$$\beta_2=2\omega_b^{-1}\tanh^{-1}(\tanh\beta_1\omega_a/2-2\mu^2/\tau_b) \tag{19}$$

$$\beta_4=2\omega_a^{-1}\tanh^{-1}(\tanh\beta_3\omega_b/2-2\mu^2/\tau_a) \tag{20}$$

Using Eq. (14), one obtains the work input in the adiabatic processes

$$W_{12}=\int_0^{\tau_b}\mathrm{d}E_S=(\omega_b-\omega_a)(\frac{S_1}{\hbar}+\frac{\mu^2}{2\tau_a})+\frac{\mu^2(\omega_a+\omega_b)}{2\tau_a} \tag{21}$$

$$W_{34}=\int_0^{\tau_a}\mathrm{d}E_S=(\omega_a-\omega_b)(\frac{S_3}{\hbar}+\frac{\mu^2}{2\tau_b})+\frac{\mu^2(\omega_a+\omega_b)}{2\tau_b} \tag{22}$$

(4). The bypass heat leakage

The heat reservoirs both are harmonic oscillator system. The harmonic oscillator system obeys the Bose-Einstein distribution law and population of the oscillator is given by $n_c=1/(e^{\hbar\omega_c\beta_c}-1)$. Similar to the derivation of $\dot{S}$ in above section, one can derive [27]

$$\dot{n}_c=-2ce^{\lambda\hbar\beta_h\omega_c}[(e^{\hbar\beta_h\omega_c}-1)n_c-1] \tag{23}$$

where λ and c are constants. According to thermodynamics of harmonic oscillator system [23], one obtains

$$\dot{Q}_e=C_e\hbar\omega_c\dot{n}_c=2C_ec\hbar\omega_ce^{\lambda\hbar\beta_h\omega_c}[1-(e^{\hbar\beta_h\omega_c}-1)n_c] \tag{24}$$

According to assumption for heat reservoirs mentioned above, $\dot{Q}_e$ is assumed to be constant, and one obtains

$$Q_e=\dot{Q}_e\tau=2C_ec\hbar\omega_ce^{\lambda\hbar\beta_h\omega_c}[1-(e^{\hbar\beta_h\omega_c}-1)n_c]\tau \tag{25}$$

CYCLE PERIOD

For the isomagnetic braches, the duration of them can be calculated from Eq. (10) and is given by $\tau_{if}=\int_{S_i}^{S_f}\mathrm{d}S/\dot{S}$, so that, one can obtain the duration of processes $4\to1$ and $2\to3$, respectively

$$\tau_h=\int_{S_4}^{S_1}\mathrm{d}S/\dot{S}=\frac{\left\{\begin{matrix}\ln[\tanh(\beta_h\omega_a/2)-\tanh(\beta_3\omega_b/2)+2\mu^2/\tau_a]\\-\ln[\tanh(\beta_h\omega_a/2)-\tanh(\beta_1\omega_a/2)]\end{matrix}\right\}}{2a\hbar^2e^{q\beta_h\omega_a}(e^{\beta_h\omega_a}+1)} \tag{26}$$

$$\tau_c=\int_{S_2}^{S_3}\mathrm{d}S/\dot{S}=\frac{\left\{\begin{matrix}\ln[\tanh(\beta_c\omega_b/2)-\tanh(\beta_1\omega_a/2)+2\mu^2/\tau_b]\\-\ln[\tanh(\beta_c\omega_b/2)-\tanh(\beta_3\omega_b/2)]\end{matrix}\right\}}{2a\hbar^2e^{q\beta_c\omega_b}(e^{\beta_c\omega_b}+1)} \tag{27}$$

Simply, one obtains the cycle period by adding the duration of the four branches of the cycle

$$\tau=\tau_h+\tau_c+\tau_a+\tau_b \tag{28}$$

OPTIMAL HEATING LOAD AND COP PERFORMANCE

(1). General case

Along two isomagnetic branches, the field is constant so that there is no work input. Therefore, the total work input per cycle is equal to the work input in the two adiabatic branches and can be calculated from Eqs. (21) and (22)

$$W_{in}=0.5(\omega_a-\omega_b)[\tanh(\beta_1\omega_a/2)-\tanh(\beta_3\omega_b/2)]+\mu^2(\omega_a/\tau_b+\omega_b/\tau_a) \tag{29}$$

Using Eqs. (15), (25) and (28), one obtains heating load and COP

$$\pi=0.5\omega_a[\tanh(\beta_1\omega_a/2)-\tanh(\beta_3\omega_b/2)+2\mu^2/\tau_a]\tau^{-1}-2C_ec\hbar\omega_ce^{\lambda\hbar\beta_h\omega_c}[1-(e^{\hbar\beta_h\omega_c}-1)n_c] \tag{30}$$

$$\psi=\frac{\left\{\begin{matrix}\omega_a[\tanh(\beta_1\omega_a/2)-\tanh(\beta_3\omega_b/2)+2\mu^2/\tau_a]\\-4C_ec\hbar\omega_ce^{\lambda\hbar\beta_h\omega_c}[1-(e^{\hbar\beta_h\omega_c}-1)n_c]\tau\end{matrix}\right\}}{\left\{\begin{matrix}(\omega_a-\omega_b)[\tanh(\beta_1\omega_a/2)-\tanh(\beta_3\omega_b/2)]\\+2\mu^2(\omega_a/\tau_b+\omega_b/\tau_a)\end{matrix}\right\}} \tag{31}$$

Both of π and ψ are functions of β_1 and β_3. By using numerical calculations, one plots Figs. 2 and 3 which display the relation of $\pi/\pi_{\max,\mu=0,C_e=0}$ versus β_1, β_3 and ψ versus β_1, β_3, and $\pi_{\max,\mu=0,C_e=0}$ is the maximum of π with $\mu=0$ and $C_e=0$. According to Refs. [27, 29, 41], the parameters are set as $\beta_h=0.5$, $\beta_c=1$, $a=c=2$, $q=\lambda=-0.5$, $\tau_a=\tau_b=0.01$, $\omega_a=8$, $\omega_b=2$, $\omega_c=0.4$, $\mu=0.003$ and $C_e=0.05$ in the numerical calculations, and for simplicity, $\hbar=1$ and $k_B=1$ are

set. Fig. 2 displays that the heating load has a maximum ($\pi_{\max}$). That is similar to that of a quantum spin Carnot heat pump [41], however, a quantum harmonic Carnot heat pump has no maximum heating load [42]. This difference indicates that the quantum characteristics of the working substance does affect the performance and cannot be neglected. Fig. 3 displays that, the ψ also has a maximum ($\psi_{\max}$) with nonzero corresponding heating load with $C_e \neq 0$.

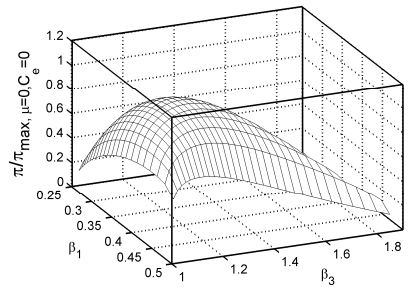

Figure 2 $\pi/\pi_{\max,\mu=0,C_e=0}$ versus β_1 and β_3

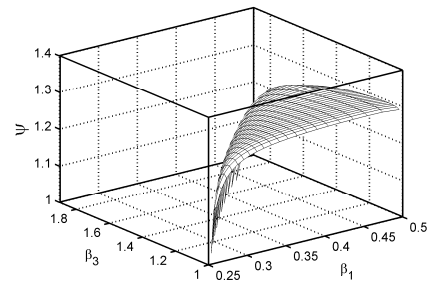

Figure 3 ψ versus β_1 and β_3

To optimize the performance, one introduces Lagrangian functions as $L_a = \pi + \lambda_a \psi$ or $L_b = \psi + \lambda_b \pi$, where λ_a and λ_b are two the Lagrangian multipliers. Combining Eqs. (30), (31) and the Euler-Lagrange equations

$$\partial L_a / \partial \beta_1 = 0,\ \partial L_a / \partial \beta_3 = 0 \tag{32}$$

or

$$\partial L_b / \partial \beta_1 = 0,\ \partial L_b / \partial \beta_3 = 0 \tag{33}$$

gives the optimal relation between the β_1 and β_3. Using this relation, one obtains the optimal $\pi - \psi$ relationship. However, the Euler-Lagrange equations are so complex and nonlinear that one can't solve them analytically and obtain the analytical optimal relationship. Using the parameters as those used in the calculation for Fig. 2 except for μ and C_e, one can solve these equations numerically and plot the $\pi/\pi_{\max,\mu=0,C_e=0} - \psi$ characteristic curves, as displayed in Fig. 4. Fig. 4 displays that, for given ω_b/ω_a, the $\pi/\pi_{\max,\mu=0,C_e=0} - \psi$ curve is a beeline and ψ is constant for the endoreversible case, i.e. $\mu = 0$ and $C_e = 0$. The heat leakage changes $\pi/\pi_{\max,\mu=0,C_e=0} - \psi$ curve to a monotonic increasing one, while the quantum friction changes it to a parabolic-like one. For the case $C_e \neq 0,\ \mu \neq 0$, the $\pi/\pi_{\max,\mu=0,C_e=0} - \psi$ curve changes to a loop-shaped one and both π and ψ have maximum. Fig. 4 also displays that, for given π, the quantum friction and heat leakage both decreases $\psi_{\max}$. The quantum friction makes the $\pi_{\max}$ increase, and this increase originates from the increase of power input due to the existence of quantum friction. The quantum friction and heat leakage both affect $\pi/\pi_{\max,\mu=0,C_e=0} - \psi$ characteristics not only quantitatively but also qualitatively.

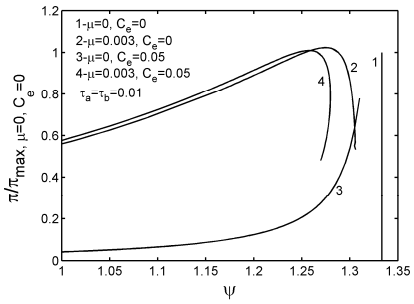

Figure 4 $\pi/\pi_{\max,\mu=0,C_e=0}$ versus ψ

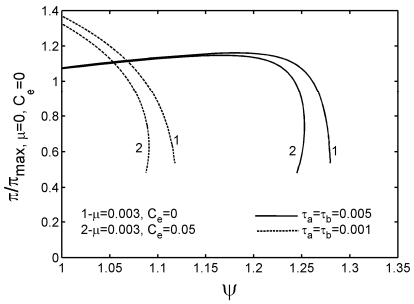

Figure 5 Effects of τ_a and τ_b on $\pi/\pi_{\max,\mu=0,C_e=0}$ versus ψ

To analyse the effects of adiabatic process time (τ_a, τ_b) on the performance, one plots Fig. 5 that display the $\pi - \psi$ characteristic curves with $\tau_a = \tau_b = 0.005$ and $\tau_a = \tau_b = 0.001$. The other parameters used in calculation are same as those used in calculations for lines 2 and 4 in Fig. 4. Comparing Figs. 5 with 4, one obtains that, with $\tau_a = \tau_b = 0.005$, the characteristic curves are only quantitatively different from that with $\tau_a = \tau_b = 0.01$. However, as τ_a and τ_b decrease to 0.001, the characteristic curves are monotonic decreasing or parabolic-like, respectively, for the case without or with heat leakage. That is quantitatively different form that with $\tau_a = \tau_b = 0.01$. Eq. (14) shows that as the duration of the adiabatic process decreases, the dissipation of work along adiabatic process increases. This part of work is pumped to hot reservoir finally which makes π increase. When the duration of the adiabatic process is short enough, such as $\tau_a = \tau_b = 0.001$, the effects of quantum friction is very strong and most of heat pumped to the hot reservoir is work dissipation, and as a result, the pump has small ψ.

(2). The case at high temperature limit

For the case $\beta_j \omega_k \ll 1$ ($j = 1, 3, h, c$, $\omega = a, b, c$), i.e. the temperatures are high enough, the obtained result above can by simplified. Eqs. (15), (24), (28) and (29) are, respectively, simplified to

$$Q_{41} = \omega_a(\beta_1\tau_a\omega_a - \beta_3\tau_a\omega_b + 4\mu^2)/(4\tau_a) \quad (34)$$

$$\dot{Q}_e \approx C_e 2c\hbar\omega_c(1+\lambda\hbar\beta_h\omega_c)(\beta_c-\beta_h)\beta_c^{-1} = C_e\alpha(\beta_c-\beta_h) \quad (35)$$

$$\tau = \frac{1}{4a\hbar^2}\ln\frac{\left[\begin{matrix}(\beta_h\tau_a\omega_a - \beta_3\tau_a\omega_b + 4\mu^2)\\(\beta_c\tau_b\omega_b - \beta_1\tau_b\omega_a + 4\mu^2)\end{matrix}\right]}{\tau_a\omega_a\tau_b\omega_b(\beta_h-\beta_1)(\beta_c-\beta_3)} + \tau_a + \tau_b \quad (36)$$

$$W_{in} = \frac{4\mu^2(\omega_a\tau_a+\omega_b\tau_b) + \tau_a\tau_b(\omega_a-\omega_b)(\beta_1\omega_a-\beta_3\omega_b)}{4\tau_a\tau_b} \quad (37)$$

Using Eqs. (34)-(37), one simplifies the heating load and COP to

$$\pi = \frac{a\hbar^2\omega_a(\beta_1\tau_a\omega_a - \beta_3\tau_a\omega_b + 4\mu^2)}{\left\{\begin{matrix}\tau_a\ln(\beta_h\tau_a\omega_a - \beta_3\tau_a\omega_b + 4\mu^2)\\-\ln[\tau_a\omega_a\tau_b\omega_b(\beta_c-\beta_3)(\beta_h-\beta_1)]\\+\ln(\beta_c\tau_b\omega_b - \beta_1\tau_b\omega_a + 4\mu^2)\\+4\tau_a a\hbar^2(\tau_a+\tau_b)\end{matrix}\right\}} - C_e\alpha(\beta_c-\beta_h) \quad (38)$$

$$\psi = \frac{\left\{\begin{matrix}a\hbar^2\tau_b\omega_a(\beta_1\tau_a\omega_a + 4\mu^2 - \beta_3\tau_a\omega_b) - \tau_a\tau_b C_e\alpha(\beta_c-\beta_h)\\\times\left\{\begin{matrix}\ln(\beta_c\tau_b\omega_b + 4\mu^2 - \beta_1\tau_b\omega_a) + 4a\hbar^2(\tau_a+\tau_b)\\+\ln(\beta_h\tau_a\omega_a + 4\mu^2 - \beta_3\tau_a\omega_b)\\-\ln[\tau_a\omega_a\tau_b\omega_b(\beta_h-\beta_1)(\beta_c-\beta_3)]\end{matrix}\right.\end{matrix}\right\}}{a\hbar^2\tau_a\tau_b(\beta_1\omega_a-\beta_3\omega_b)(\omega_a-\omega_b) + 4a\hbar^2\mu^2(\omega_a\tau_a+\omega_b\tau_b)} \quad (39)$$

where $\alpha = 2c\hbar\omega_c(1+\lambda\hbar\beta_h\omega_c)/\beta_c$.

Similar to general case, one can plots three-dimensional diagrams of $\pi/\pi_{\max,\mu=0,C_e=0}$ and ψ by using numerical calculations, but for simplicity, the figures are not given in this paper. The calculations show that, at high temperature limit, three-dimensional diagrams of π and ψ versus temperatures β_1 and β_3 are similar to that for general case.

Similarly, to determine the optimal $\pi-\psi$ performance, one introduces Lagrangian functions $L_c = \pi + \lambda_c\psi$ or $L_d = \psi + \lambda_d\pi$, where λ_c and λ_d are two Lagrangian multipliers. Combining Eqs. (38), (39) and Euler-Lagrange equations

$$\partial L_c/\partial\beta_1 = 0,\ \partial L_c/\partial\beta_3 = 0 \quad (40)$$

or

$$\partial L_d/\partial\beta_1 = 0,\ \partial L_d/\partial\beta_3 = 0 \quad (41)$$

one can optimize the performance, however, at high temperature limit, the Euler-Lagrange equations are still nonlinear and too complex, one cannot solve them analytically. Using numerical calculations, one plots Fig. 6 with $\tau_a = \tau_b = 0.01$ and Fig. 7 with $\tau_a = \tau_b = 0.005$ and $\tau_a = \tau_b = 0.001$ which display the characteristic curves of the $\pi/\pi_{\max,\mu=0,C_e=0}$ versus ψ at high temperature. Parameters used herein are set as $a = c = 2$, $q = \lambda = -0.5$, $\beta_h = 1/290$, $\beta_c = 1/260$, $\omega_a = 12$, $\omega_b = 8$, $\omega_c = 6$, and for simplicity, $\hbar = 1$ and $k_B = 1$ are also set. Comparisons among Figs. 4, 6 and 7 show that, for $\pi-\psi$ characteristic, there is only quantitative difference between the two cases.

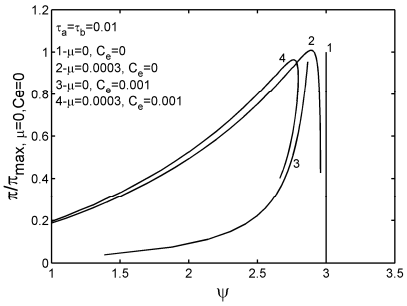

Figure 6 $\pi/\pi_{\max,\mu=0,C_e=0}$ versus β_1 and β_3 with $\tau_a = \tau_b = 0.01$ at high temperature limit

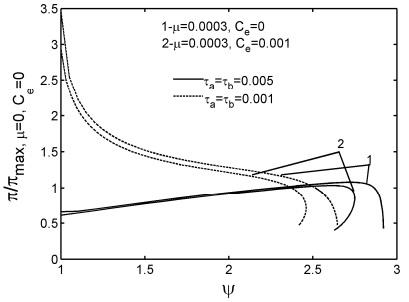

Figure 7 Effects of τ_a and τ_b on $\pi/\pi_{\max,\mu=0,C_e=0}$ versus ψ at high temperature limit

CONCLUSION

By considering quantum friction, heat resistance and heat leakage, this paper establishes a Brayton heat pump cycle model. By combining quantum thermodynamics and quantum master equation, this paper obtains the heating load and COP and optimal performance. By using the Euler-Lagrange method, one optimizes heating load and COP performance for two cases: the general case and the case at high temperature limit. Also, influences of quantum friction, duration of the adiabatic process and heat leakage on the performance are further analyzed.

The results show that, in general case, the π-ψ characteristic curve is a beeline when the cycle is endoreversible. The existence of quantum friction makes the characteristic curve a parabolic-like one while the bypass heat leakage makes it a monotonic increasing one. When there exist heat resistance, quantum friction and heat leakage, characteristic curve is a loop-shaped one. As the duration of adiabatic process is short enough, affected strongly by the quantum friction, the characteristic curves change into monotonic decreasing one or parabolic-like one for case without or with heat leakage, respectively. For the two cases, i.e. at high temperature limit and in general case, the optimal performance are similar.

ACKNOWLEDGMENT

This paper is supported by the Natural Science Fund of China (Project No. 51576207) and the Innovation Research

Foundation for Ph. D Candidates of Naval University of Engineering (HGBSJJ2012002).

REFERENCES

[1] Bejan A., Entropy Generation through Heat and Fluid Flow, New York: Wiley, 1982.

[2] Andresen B., Finite-Time Thermodynamics, Physics Laboratory Ⅱ, University of Copenhagen, 1983.

[3] Chen L.G., Finite-Time Thermodynamic Analysis of Irreversible Processes and Cycles (in Chinese), Beijing: Higher Education Press, 2005.

[4] Feidt M., Thermodynamics of energy systems and processes: A review and perspectives, *J. Appl. Fluid Mech.*, Vol. 5, 2012, pp. 85-98.

[5] Bejan A., Entropy generation minimization, exergy analysis, and the constructal law, *Ara. J. Sci. Eng.*, Vol. 38, 2013, pp. 329-340.

[6] Chen L.G., Meng F.K., and Sun F.R., Thermodynamic analyses and optimizations for thermoelectric devices: the state of the arts. *Sci. China: Tech.*, Vol. 59, 2016, pp. 442-455.

[7] Ge Y.L., Chen L.G., and Sun F.R., Progress in finite time thermodynamic studies for internal combustion engine cycles, *Entropy*, Vol. 18, 2016, pp. 139.

[8] Chen L.G., and Xia S.J., Generalized Thermodynamic Dynamic-Optimization for Irreversible Cycles (in Chinese), Beijing: Science Press, 2017.

[9] Chen L.G., and Xia S.J., Generalized Thermodynamic Dynamic-Optimization for Irreversible Processes (in Chinese), Beijing: Science Press, 2017.

[10] Bi Y.H., and Chen L.G., Finite Time Thermodynamic Optimization for Air Heat Pumps (in Chinese), Beijing: Science Press, 2017.

[11] Sieniutycz S., and Tsirlin A., Finding limiting possibilities of thermodynamic systems by optimization, *Philos. Trans. Roy. Soc. A*, 2017, Vol. 375, pp. 20160219.

[12] Blanchard C. H., Coefficient of performance for finite-speed heat pump, *J. Appl. Phys*., Vol. 51, 1980, pp. 2471-2472.

[13] Feng H.J., Chen L.G., Sun F.R., and Wu C., Heating load and COP Optimizations for a universal steady flow endoreversible heat pump model, *Int. J. Ambient Energy*, Vol. 32, 2011, pp. 70-77.

[14] Chen L.G., Wu C., and Sun F.R., Heat transfer effect on specific heating load of heat pumps, *Appl. Thermal Eng*., Vol. 17, 1997, pp. 103-110.

[15] Zhu X.Q., Chen L.G., and Sun F.R., Optimal performance of a generalized irreversible Carnot heat pump with a generalized heat transfer law, *Phys. Scr.*, 64, 2001, pp. 584-587.

[16] Angelino G., and Invernizzi C., Prospects for real-gas reversed Brayton cycle heat pumps, *Int. J. Refrig.*, Vol. 18, 1995, pp. 272-280.

[17] Bi Y.H., Chen L.G., and Sun F.R., Comparative performance analysis for endoreversible simple air heat pump cycles considering ecological, exergetic efficiency and heating load objectives, *Int. J. Exergy*, Vol. 6, 2009, pp. 550-566.

[18] Chen J., and Yan Z., Equivalent combined systems of three-heat-source heat pumps, *J. Chem. Phys.*, Vol. 90, 1989, pp. 4951-4955.

[19] Qin X.Y., Chen L.G., Ge Y.L., and Sun F.R., Thermodynamic modeling and performance analysis of variable-temperature heat reservoir absorption heat pump cycle, *Physica A*, Vol. 436, 2015, pp. 788-797.

[20] Wu C., and Schulden W., Specific heating load of thermoelectric heat pumps, *Energy Convers. Manage.*, Vol. 35, 1994, pp. 459-464.

[21] Meng F.K., Chen L.G., and Sun F.R., Extreme working temperature differences for thermoelectric refrigerating and heat pumping devices driven by thermoelectric generator, *J. Energy Inst.*, Vol. 83, 2010, pp. 108-113.

[22] van den Broek M., and van den Broeck C., Chiral Brownian heat pump, *Phys. Rev. Lett.*, Vol. 100, 2008, pp. 130601.

[23] Ding Z.M., Chen L.G., and Sun F.R., Thermodynamic characteristic of a Brownian heat pump in a spatially periodic temperature field, *Sci. China Phys. Mech. Astron.*, Vol. 53, 2010, pp. 876-885.

[24] He J., and He X., Energy selective electron heat pump with transmission probability (in Chinese), *Acta. Phys. Sin.*, Vol. 59, 2010, pp. 2345-2349.

[25] Ding Z.M., Chen L.G., Ge Y.L., and Sun F.R., Performance optimization of total momentum filtering double-resonance energy selective electron heat pump, *Physica A*, Vol. 447, 2016, pp. 49-61.

[26] Scoail H., and Schula-Dubois E., Three-level masers as engines, *Phys. Rev. Lett.*, Vol. 2, 1959, pp.262-263.

[27] Geva E., and Kosloff R., On the classical limit of quantum thermodynamics in finite time, *J. Chem. Phys.*, Vol. 97, 1992, pp. 4398-4412.

[28] Wu F., Chen L.G., Sun F.R., Wu C., and Zhu Y., Performance and optimization criteria of forward and reverse quantum Stirling cycles, *Energy Convers. Manage*., Vol. 39, 1998, pp. 733-739.

[29] Feldmann T., and Kosloff R., Performance of discrete heat engines and heat pumps in finite time, *Phys. Rev. E*, Vol. 61, 2000, pp. 4774-4790.

[30] Wu F., Chen L.G., Sun F.R., and Wu C., Performance of an irreversible quantum Carnot engine with spin-1/2, *J. Chem. Phys.*, Vol. 124, 2006, pp. 214702.

[31] Kosloff R., Quantum thermodynamics: A dynamical viewpoit. *Entropy*, Vol. 15, 2013, pp. 2100-2128.

[32] Feldmann T., and Kosloff R., Short time cycles of purely quantum refrigerator, *Phys. Rev. E*, Vol. 85, 2012, pp. 051114.

[33] Chen L.G., Liu X.W., Ge Y.L., Wu F., and Sun F., Ecological optimisation of an irreversible harmonic oscillators Carnot refrigerator, *J. Energy Inst.,* Vol. 86, 2013, pp. 85-96.

[34] Liu X.W., Chen L.G., Wu F., and Sun F.R., Optimal performance of a spin quantum Carnot heat engine with multi-irreversibilities, *J. Energy Inst.*, Vol. 87, 2014, pp. 69-80.

[35] Liu X.W., Chen L.G., Wu F., and Sun F.R., Optimal fundamental characteristic of a quantum harmonic oscillator Carnot refrigerator with multi-irreversibilities, *Int. J. Energy Environ.*, Vol. 6, 2015, pp. 537-552.

[36] Yin Y. Chen L.G., and Wu F., Optimal power and efficiency of quantum Stirling heat engines, *Eur. Phys. J. Plus*, Vol. 132, 2017, pp. 45.

[37] Wu F., Chen L.G., and Sun F.R., Ecological optimum performance of a spin-1/2 quantum heat pump (in Chinese), *J. Naval Academy Eng.*, 1996, No. 4, pp. 1-6.

[38] Wu F., Sun F.R., and Chen L.G., Optimal performance parameters of a harmonic oscillation quantum Carnot heat pump (in Chinese), *J. Eng. Thermal Energy Pow.*, Vol. 12, 1997, pp. 361-364.

[39] Lin B., and Chen J., Performance analysis of a quantum heat-pump using spin systems as the working substance, *Appl. Energy*, Vol. 78, 2004, pp. 75-93.

[40] Lin B., and Chen J., General performance characteristics of a quantum heat pump cycle using harmonic oscillators as the working substance, *Phys. Scr.*, Vol. 71, 2005, pp. 12-19.

[41] Liu X.W., Chen L.G., Wu F., and Sun F.R., Fundamental optimal relation of an irreversible quantum Carnot heat pump with spin-1/2 systems, *Math. Comput. Model.*, Vol. 54, 2011, pp. 190-202.

[42] Liu X.W., Chen L.G., Wu F., and Sun F.R., Fundamental optimal relation of a generalized irreversible quantum Carnot heat pump with harmonic oscillators, *Int. J. Ambient Energy*, Vol. 33, 2012, pp. 118-129.

[43] Zeng J., Quantum Mechanics (in Chinese), 3 ed. Beijing: Science Press, 2000.

[44] Kosloff R., Ratner M. A., and Davis W. B., Dynamics and relaxation in interacting systems: Semigroup methods. *J. Chem. Phys.*, Vol. 106, 1997, pp. 7036-7043.